minerals

MDPI

Article

Mineralogical Characteristics of Late Permian Coals from the Yueliangtian Coal Mine, Guizhou, Southwestern China

Panpan Xie *, Hongjian Song, Jianpeng Wei and Qingqian Li

College of Geoscience and Surveying Engineering, China University of Mining and Technology, Beijing 100083, China; songhongjian90@gmail.com (H.S.); weijianpeng15@gmail.com (J.W.); liqingqian7@gmail.com (Q.L.)
* Correspondence: xiepanpan91@gmail.com; Tel.: +86-10-6234-1868

Academic Editor: Thomas Kerestedjian
Received: 6 December 2015; Accepted: 16 March 2016; Published: 31 March 2016

Abstract: This paper reports the mineralogical compositions of super-low-sulfur (Yueliangtian 6-upper (YLT6U)) and high-sulfur (Yueliangtian 6-lower (YLT6L)) coals of the Late Permian No. 6 coal seam from the Yueliangtian coal mine, Guizhou, southwestern China. The mineral assemblages and morphology were detected and observed by X-ray diffractogram (XRD), optical microscopy and field-emission scanning electron microscope (FE-SEM) in conjunction with an energy-dispersive X-ray spectrometer. Major minerals in the coal samples, partings and host rocks (roof and floor strata) include calcite, quartz, kaolinite, mixed-layer illite/smectite, chlorite and pyrite and, to a lesser extent, chamosite, anatase and apatite. The Emeishan basalt and silicic rocks in the Kangdian Upland are the sediment source for the Yueliangtian coals. It was found that there are several modes of chamosite occurrence, and precursor minerals, such as anatase, had been corroded by Ti-rich hydrothermal solutions. The modes of occurrence of minerals present in the coal were controlled by the injection of different types of hydrothermal fluids during different deposition stages. The presence of abundant pyrite and extremely high total sulfur contents in the YLT6L coal are in sharp contrast to those in the YLT6U coal, suggesting that seawater invaded the peat swamp of the YLT6L coal and terminated at the YLT6U-9p sampling interval. High-temperature quartz, vermicular kaolinite and chloritized biotite were observed in the partings and roof strata. The three partings and floor strata of the No. 6 coal seam from the Yueliangtian coal mine appear to have been derived from felsic volcanic ash. Four factors, including sediment-source region, multi-stage injections of hydrothermal fluids, seawater influence and volcanic ash input, were responsible for the mineralogical characteristics of the Yueliangtian coals.

Keywords: minerals; coal; hydrothermal fluids; seawater influence; tonstein

1. Introduction

Guizhou province in southwestern (SW) China contains abundant coal resources. The Late Permian coals from western Guizhou province have attracted much attention [1–5], not only because of the coal-hosted rare-metal ore deposits found in this area [6–8], but also due to their mineralogical and geochemical indications for the reginal geology evolution, such as the mantle plume formation located to the west of the coal basin [1,3]. Practically, although Panxian county is closely located to the high-incidence area of the endemic arsenosis and fluorosis in SW China, the relation between mineralogical compositions of the coals in this area and the endemic disease occurring in the surrounding areas is unknown. The Yueliangtian coal mine in Panxian county provides large-scale energy resources for its region, and the coals are directly used for combustion, despite high mineral contents in these coals, as described below. Thus, it is necessary to determine the contents and modes

of occurrence of minerals in coals for the environmental issues caused by coal combustion in the area. Theoretically, mineral matter in coal may indicate depositional environments during peat accumulation, as well as geological processes during diagenetic and epigenetic stages [9]. Although the coals in Panxian county of southwestern Guizhou province have been reported by a few researchers [4,5], geochemical characteristics, modes of mineral occurrence and their controlling geological factors in these coals, however, have not been well addressed. In this paper, we report the mineralogical characteristics of the Late Permian coals from the No. 6 coal seam at the Yueliangtian coal mine, Guizhou, SW China.

2. Geological Setting

The Yueliangtian coal mine is located in Panxian county, western Guizhou, southwestern China, covering a total area of around 15 km^2, 6 km N–S long and 2.5 km W–E wide (Figure 1). Tectonically, the Yueliangtian deposit belongs to a monocline structure with an approximate east dip [6]. It is limited by well-developed normal faults within the epsilon-type structure in the Puan tectonic zone [6,10], covering the area between latitudes 25°54′22″ and 25°57′44″ N and longitudes 104°30′36″ and 104°31′59″ E. The Kangdian Upland is the dominant sediment-source region for this coal deposit in western Guizhou [11].

The sedimentary sequences in the Yueliangtian coal mine are the Late Permian and Early Triassic (Figure 2) strata. The Late Permian strata, with major coal resources in the area, consist of the Longtan and Emeishan Basalt Formations. The upper and lower portions of the Emeishan Basalt Formation are dominated by grey-lilac tuffs and grey-dark basalts, respectively, similar to those in the surrounding areas such as the Zhijing Coalfiled in western Guizhou [12].

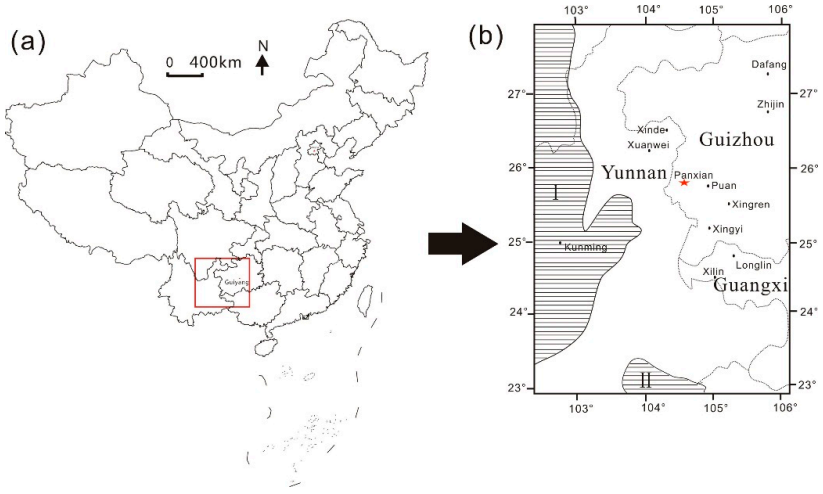

Figure 1. Location of the Yueliangtian coal mine. (**a**) China map and the location of study area; (**b**) Depositional environments during the Late Permian in Guizhou province, China. I, Kangdian Upland. II, Northern Vietnam Upland. (b) The enlargement of the red area in (a), modified from Dai *et al.* [15].

The Longtan Formation (P_{2l}) is the major coal-bearing strata of the coal mine. The sedimentary environment of the Longtan Formation varies greatly from lower delta plains, through tidal flats, to carbonate subtidal flats [11–14]. As shown in Figure 2, the upper portion of the Longtan Formation (81.97 m) is made up of siltstone, siderite layers and twelve coal seams. Its middle portion (89.75 m), intercalated with siderite layers and coal beds, is mainly composed of siltstone and silty mudstone. A total of 16 coal beds occur in the middle portion. The lower portion is composed of siltstone, silty mudstone, pelitic siltstone, siderite and ten coal seams. The Yueliangtian 6-upper (YLT6U) and 6-lower (YLT6L) coals, separated by a gray siltstone (2.94 m) that contains siderite layers and plenty

of plant-root fossils, occur in the upper portion of the Longtan Formation. Currently, the YLT6U coal seam is the only mineable seam in this area (Figure 2).

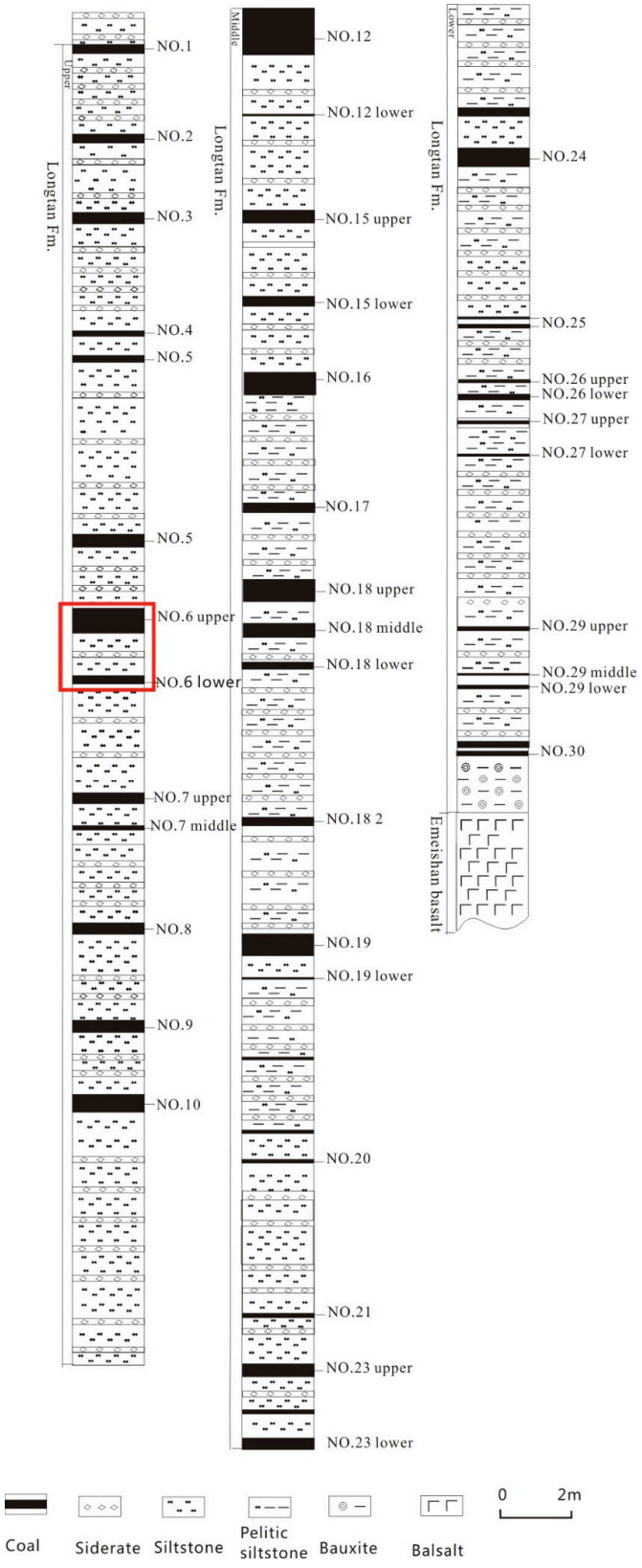

Figure 2. Sedimentary sequences and coal seams (red area) in the Yueliangtian coal mine.

3. Sample Collection and Analytical Procedures

According to Chinese Standard Method GB/T 482-2008 [16], a total of nineteen bench samples were collected from the No. 6 coal seam (YLT6) in the underground workings of the Yueliangtian coal mine in Panxian county, western Guizhou. The floor of the YLT6U coal and the roof of the YLT6L coal are unavailable, due to the complex structure, as well as limited capacity in sample collection. From top to bottom, the roof strata (with suffix-r), coal benches, partings (with suffix-p) and floor-stratum samples (with suffix-f) are identified, with the coal seams numbered in increasing order from top to bottom (Figure 3). Each bench sample was immediately stored in a clean and uncontaminated plastic bag, to ensure as little contamination and oxidation as possible. The thickness of each sample is given in Table 1.

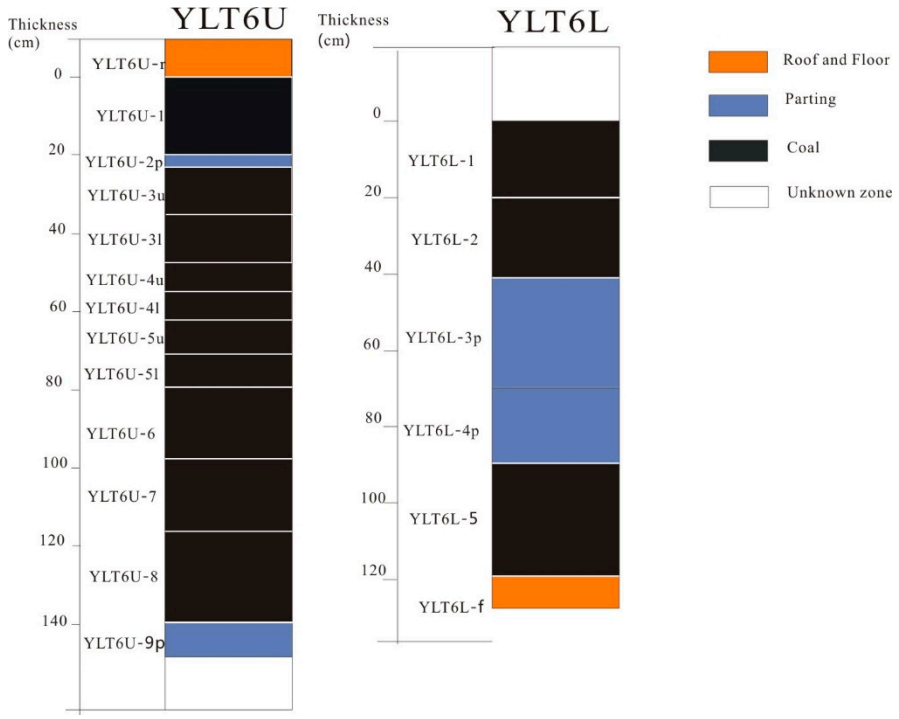

Figure 3. Lithologic column sections of the Yueliangtian 6-upper (YLT6U) and 6-lower (YLT6L) coal seams.

The samples were crushed and ground to pass the 75-μm sieve prior to analysis. In accordance with ASTM Standards D3173-11, D3175-11 and D3174-11 [17–19], proximate analysis, covering moisture and volatile matter percentages and ash yield, was conducted. Total sulfur was determined based on ASTM Standard D3177-02 [20]. The percentages of C, H and N in the coals were determined by an elemental analyzer (vario MACRO). Coarse-crushed samples of each coal were prepared as grain mounts and examined with 50× oil immersion for microscopic analysis. Following ASTM Standards D2797/D2797M-11a and D2798M-11a [21,22], vitrinite random reflectance (Rr, %) was determined using a Leica DM-4500P microscope (at a magnification of 500×) equipped with a Craic QDI 302™ spectrophotometer (Leica Inc., Wetzlar, Germany). An X-ray diffractogram (XRD) was used to determine the mineralogical compositions. Prior to XRD analysis, the low-temperature ashing (LTA) of coal was performed using an EMITECH K1050X plasma asher (Quorum Inc., Lewes, UK). A commercial interpretation software Siroquant™ [23,24] was used to obtain mineral contents in the LTAs and non-coal samples based on XRD. More information illustrating the use of this technique for coal-related materials was given by Ward *et al.* [25,26], Ruan and Ward [27] and Dai *et al.* [28,29]. Following the procedures described by Dai *et al.* [15,30], a field-emission scanning electron microscope

(FE-SEM) in conjunction with an energy-dispersive X-ray spectrometer (EDAX Inc., Mahwah, NJ, USA) was used to observe modes of mineral occurrence, and also to determine the distribution of some selected elements. Samples were carbon-coated using a Quorum Q150T ES sputtering coater (Quorum Inc.) or were not coated for low-vacuum SEM working conditions (60 bar). The working distance, beam voltage, aperture and spot size of the FE-SEM-EDS was 10 mm, 20.0 kV, 6 and 4.5–5.0, respectively. The images were captured by a back-scattered electron detector (BSE).

Table 1. Coal bench thickness (cm), proximate and ultimate analyses (%), and vitrinite random reflectance (%) of the No. 6 coals in the Yueliangtian coal mine, Guizhou, China.

Sample	Thickness (cm)	Proximate Analyses (%)			Ultimate Analyses (%)				Reflectance
		M_{ad}	A_d	V_{daf}	$S_{t,d}$	C_{daf}	H_{daf}	N_{daf}	R_r
YLT6U Coal Seam									
YLT6U-1	20	0.57	36.62	41.59	0.65	83.38	5.06	1.56	1.01
YLT6U-3u	12.5	1.45	42.36	39.87	0.28	82.91	5.52	1.68	1.02
YLT6U-3l	12.5	0.72	18.71	34.63	0.61	88.37	5.35	1.76	0.95
YLT6U-4u	7.5	0.87	34.14	34.1	0.35	87.82	7.3	1.74	0.96
YLT6U-4l	7.5	1.02	10.97	35.75	0.27	87.73	4.71	1.87	0.91
YLT6U-5u	9	0.69	16	35.53	0.23	86.21	4.93	1.49	0.94
YLT6U-5l	9	0.83	10.6	36.43	0.33	86.55	4.95	1.71	0.91
YLT6U-6	19	0.7	19.09	36.19	0.36	86.42	4.17	1.44	0.91
YLT6U-7	19	0.59	26.88	37.96	0.75	92.54	4.39	1.48	0.94
YLT6U-8	24	0.84	10.07	36.29	0.49	87.93	4.78	1.77	0.8
Wa	140 *	0.79	22.78	37.24	0.48	87.04	4.97	1.61	0.93
YLT6L Coal Seam									
YLT6L-1	20	0.89	40.6	44.15	13.34	58.71	5.19	1.11	0.77
YLT6L-2	21	1.01	27.75	37.85	8.99	80.9	4.47	1.39	0.77
YLT6L-5	30	0.45	36.37	35.44	3.61	86.15	4.54	1.24	0.75
Wa	71 *	0.74	35.01	38.61	7.94	76.87	4.7	1.25	0.76

M, moisture; A, ash yield; V, volatile matter; S_t, total sulfur; C, carbon; H, hydrogen; N, nitrogen; ad, air-dried basis; d, dry basis; daf, dry and ash-free basis; R_r, random reflectance of vitrinite; Wa, weighted average for bench sample (weighted by thickness of sample interval); * total thickness.

The clay (<2 μm) fraction of rock samples was conducted based on the Chinese Industry Standard Method [31]. The sample was dissolved in 80 mL ultrapure water and isolated by ultrasonic dispersion. After 4h standing, the natural-oriented aggregate was analyzed in an air-dried state. The glycol-saturated (50 °C, 8 h) and heated (450 °C, 2.5 h) oriented aggregates were analyzed subsequently. The mineralogy of this fraction was also analyzed by XRD.

4. Result

4.1. Coal Chemistry and Vitrinite Reflectance

The vitrinite random reflectance values and the volatile matter yields of the YLT6U and YLT6L coals (Table 1) indicate a high volatile A bituminous coal in rank [32]. The ash yield of the YLT6U coal samples varies from 10.07%–42.36%, with the weighted average much lower than that of the YLT6L coal. Total sulfur contents vary greatly between the YLT6U and YLT6L coal seams (Table 1). As shown in Tables 1 and 2 the high-sulfur samples also have high percentages of pyrite (described in more detail below). Based on Chinese Standards GB/T 15224.1/2-2010 [33], the YLT6U coal is classified as a medium-ash and super-low-sulfur coal; the YLT6L coal, with its total sulfur content higher than other coals in Guizhou province [14,34], is a medium-high-ash and high-sulfur coal.

Table 2. Low-temperature ash yields (%) of coals and mineral compositions (%) of coal low-temperature ashing (LTA), partings and host rocks (%) determined by X-ray diffractogram (XRD) and Siroquant. I/S, illite/smectite.

Sample	LTA	Quartz	Kaolinite	Chlorite	Illite	I/S	Calcite	Anatase	Pyrite	Bassanite	Ankerite	Rutile	Xenotime	Muscovite	Siderite	Stibnite	Apatite
YLT6U Coal Seam																	
YLT6U-r		24.4		17.5		26	1.9	6.2						12	12		
YLT6U-1	43.8	38.1	14.8	8.5			28				10.5						
YLT6U-2p		5.4	53.7			34.7	6.2										
YLT6U-3u	48.49	30.3	53.1				16.6										
YLT6U-3l	19.95	51.2	30.8	5.6			11.1	1.3									
YLT6U-4u	36.76	64.9	25.8	6.2			3.1										
YLT6U-4l	11.76	23.5	20.6				56										
YLT6U-5u	19.35	37.3	49.4				13.4										
YLT6U-5l	12.46	6.3	17.4				76.3										
YLT6U-6	22.89	8.6	14.3				76.8	0.3									
YLT6U-7	61.43	6.7	63.9		11.3	3.5		10.7	3.9								
YLT6U-8	10.2	24.6	22.4				48.6			4.4							
YLT6U-9p		1.5	66.7			22.4		9.4									
Wa	43.82	26.6	30.8	2	1.5	0.5	34.2	1.6	0.5	0.8	1.5						
YLT6L Coal Seam																	
YLT6L-1	59.35	5.6	10.8				6.8		65			11.7					
YLT6L-2	35.11	25.4	9				15		43.6	4.2		1	1.7				
YLT6L-3p		51.8		20.4			2.4		15.9					8.1		1.5	
YLT6L-4p		4.1	35.9			44.1		10.1	5.8								
YLT6L-5	39.79	65.3		10.8			10.5		12.3	1.1							
YLT6L-f		19	33.4			34.2	3.9	8.2									1.3
Wa	43.91	36.7	5.7	4.6			10.8		36.4	1.7		3.6	0.5				

Wa, weighted average for bench sample (weighted by thickness of sample interval).

4.2. Minerals in the No. 6 Coals in the Yueliangtian Coal Mine

4.2.1. Minerals in Coal Benches

The proportions of each crystalline phase in the coal-LTA and non-coal samples identified from XRD and Siroquant are given in Table 2. The vertical concentration (%) variations of minerals, and low-temperature ash yields (%) through the No. 6 coals in the Yueliangtian coal mine are described in Figure 4. Like other Late Permian coals in western Guizhou described by Dai *et al.* [14,34,35] and Zhuang *et al.* [36], the major minerals of the YLT6U coal LTAs are mainly calcite, kaolinite and quartz, with trace amounts of chlorite and anatase. Various contents of illite, mixed-layer illite/smectite, pyrite, bassanite and ankerite also occur in a few coal benches (Table 2). The minerals in the LTA of the YLT6L coal are mainly represented by calcite, quartz and pyrite, with a lesser proportion of kaolinite, chlorite, rutile and bassanite. The LTA of sample YLT6L-2 also contains a small proportion of xenotime.

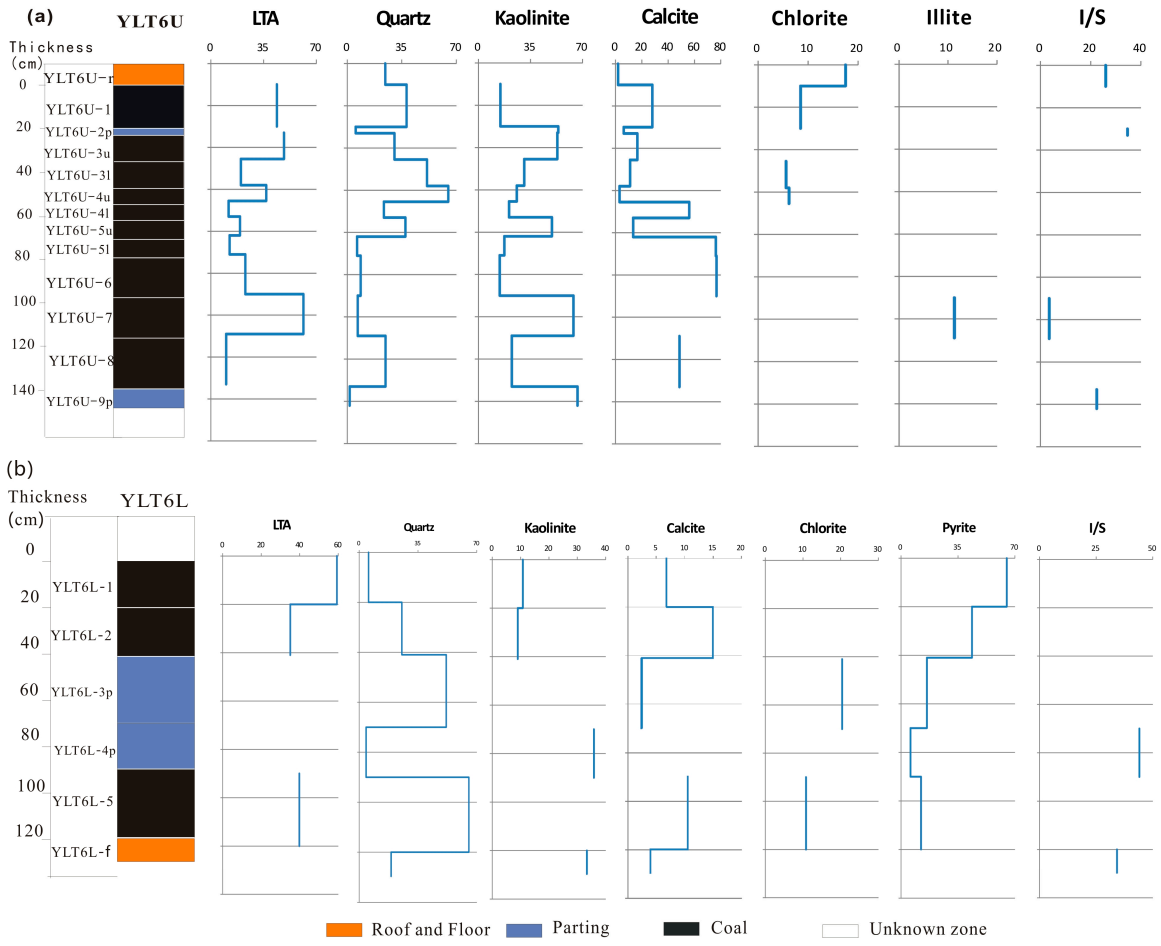

Figure 4. Concentration (%) variations of minerals and coal LTAs (%) through the No. 6 coal seam sections in the Yueliangtian coal mine. (**a**) YLT6U coal; (**b**) YLT6L coal.

Quartz in the YLT6U and YLT6L coals occurs in three forms: (1) as cell-fillings of structured inertinite macerals, suggesting an authigenic origin (Figure 5A); (2) as discrete particles embedded in collodetrinite (Figure 5B,C); and (3) coexisting with clay minerals (Figure 5D). Quartz with the latter two forms was probably derived from detrital materials of terrigenous origin.

As shown in Table 2 and Figure 4, the host rocks (roof and floor strata) and partings (YLT6U-9p and YLT6L-4p) of the YLT6U and YLT6L coals contain minor calcite. By contrast, the YLT6U coal contains abundant calcite, accounting for 76.8% of the total minerals in the LTA sample. Calcite layering

has been macroscopically observed in sample YLT6U-5l during sampling in the field. Microscopically, it occurs mainly as cell-fillings (Figure 6A), as isolated particles with various forms (Figure 6B,C) and as vein-fillings in the vitrinite (Figure 6D). A platy calcite (Figure 6B) with a large size up to 570 μm in length and 100 μm in width has distinct edges and angles.

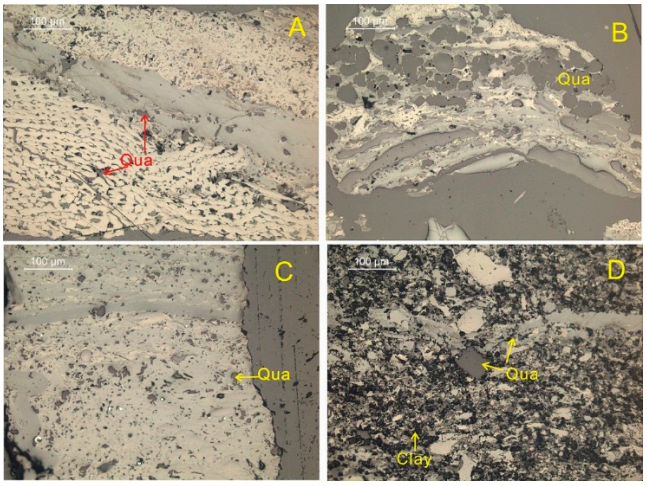

Figure 5. Quartz in the YLT6 coal (reflected white light microscopy). (**A**) Fusinite- and semifusinite-cell filling quartz in sample YLT6U-4u; (**B**) Quartz distributed along the bedding planes of sample YLT6U-4l; (**C**) Quartz embedded in collodetrinite in sample YLT6L-2; (**D**) Quartz coexisting with clay minerals in sample YLT6U-4u. Qua, quartz; Clay, clay minerals.

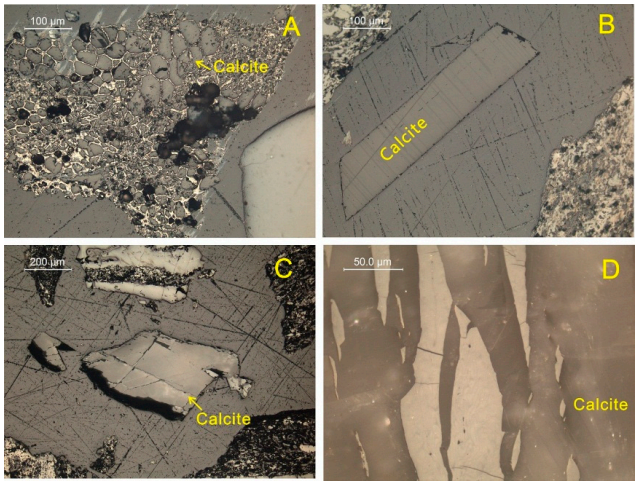

Figure 6. Calcite in the YLT6U coal (reflected white light microscope). (**A**) Cell-filling calcite in sample YLT6U-6; (**B**) calcite embedded in collodetrinite in sample YLT6U-4u; (**C**) calcite occurring as irregular shapes in sample YLT6U-1; (**D**) calcite as fracture-filling in vitrinite of sample YLT6U-1.

Kaolinite in the YLT6 coal has two modes of occurrence: as cell fillings (Figure 7A,B) and as detrital particles (Figure 5D). The former is of authigenic origin, and the latter is probably of terrigenous origin. In contrast to the minerals described above, pyrite is distributed completely differently between the YLT6U and YLT6L coals. Although below the detection limit of the XRD technique, cell-filling pyrite was observed under the optical microscope in sample YLT6U-8 (Figure 8A). Pyrites of framboidal (Figure 8B), cell-fillings (Figures 7A,B and 8C), cubic (Figure 8D) and nodular (Figure 8E) forms occur in the YLT6L coal. It is probably of syngenetic or early diagenetic origin [37–41]. Pyrite also occurs

as cleat- and fracture-fillings (Figures 7A and 8C), suggesting an epigenetic origin of hydrothermal solutions with a formation temperature around 150–200 °C [5,41,42]. Fe-S compounds with different levels of brightness (Figure 8F) deserve a special note: the atomic ratios of Fe against S of Spots 1 and 2 (Figure 8G,H) are 1:2.4 and 1:2, respectively, probably suggesting an oxidation product of pyrite in Spot 1.

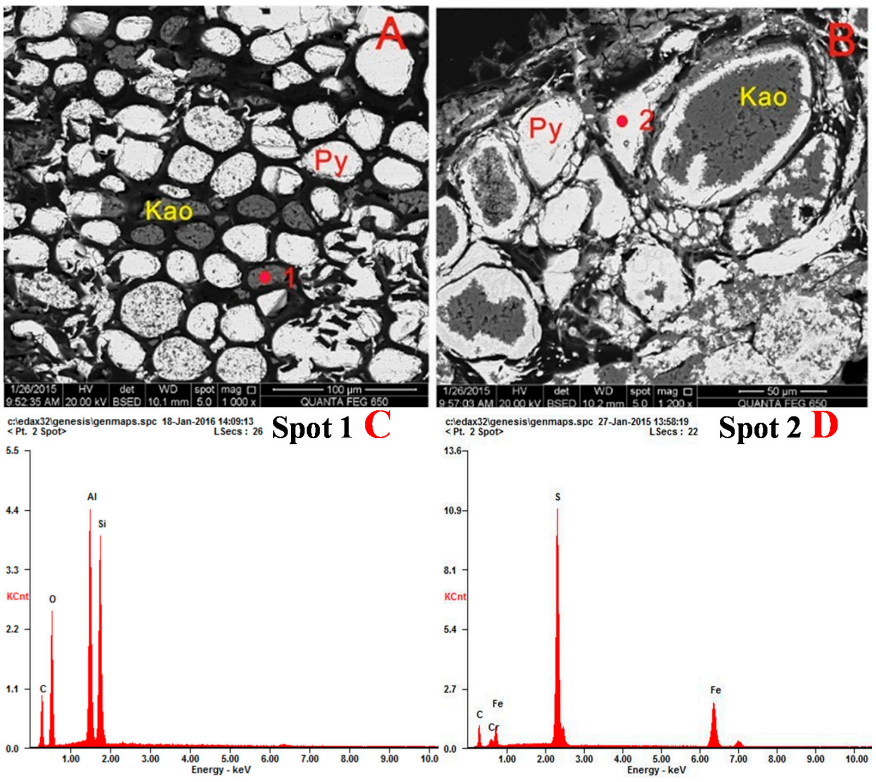

Figure 7. SEM back-scattered electron images and selected Energy Dispersive X-ray Spectroscopy (EDS) spectra of kaolinite and pyrite in YLT6L-1 coal. (**A**) Cell- and cleat-filling kaolinite and pyrite; (**B**) kaolinite and pyrite; (**C**) EDS spectrum of kaolinite; (**D**) EDS spectrum of pyrite. Kao, kaolinite; Py, pyrite.

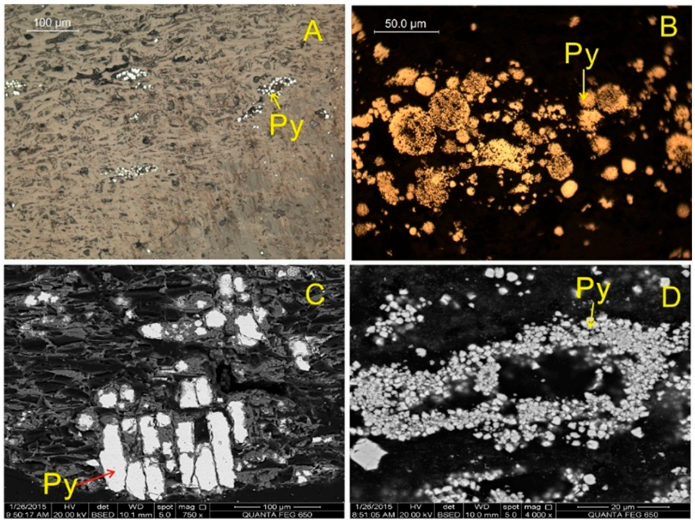

Figure 8. *Cont.*

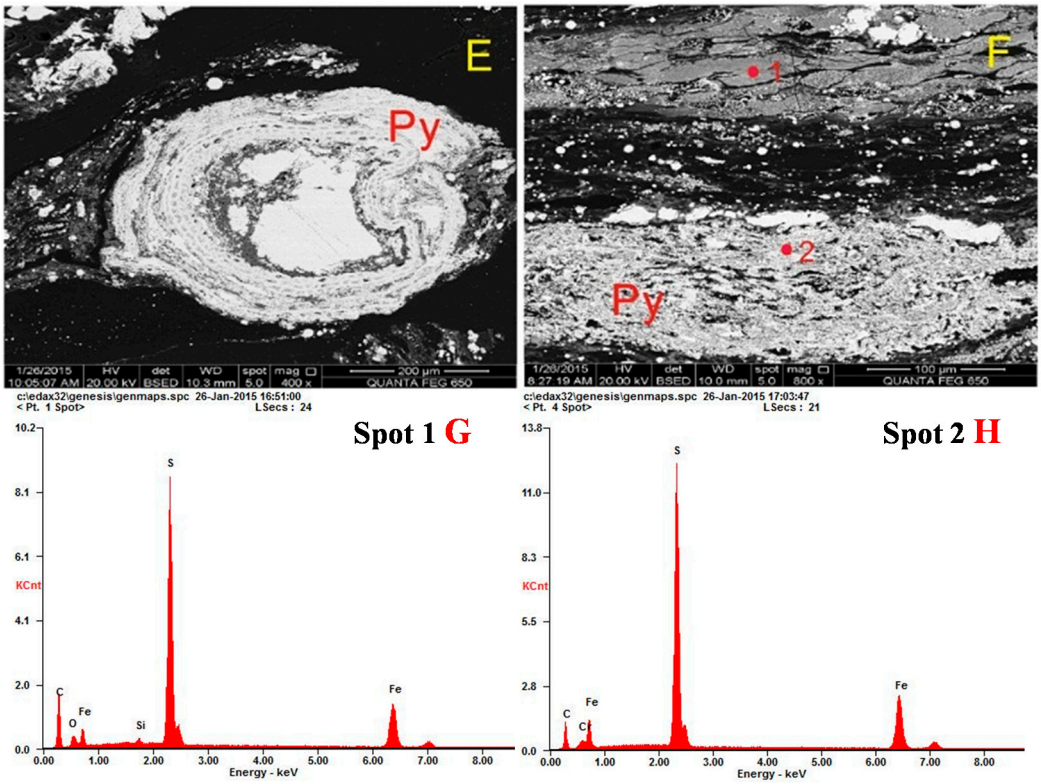

Figure 8. Reflected white light optical microscope, SEM back-scattered electron images and selected EDS data in YLT6U and YLT6L coals. (**A**) Fusinite- and semifusinite-cell filling pyrite in sample YLT6U-8 (optical microscope); (**B**) framboidal pyrite in sample YLT6L-2 (optical microscope, oil immersion); (**C**) cell- and fracture-filling pyrite in sample YLT6L-1; (**D**) cubic pyrite in sample YLT6L-1; (**E**) nodular pyrite in sample YLT6L-1; (**F**) cell-filling pyrite in sample YLT6L-1; (**G**,**H**) EDS spectra. Py, pyrite.

4.2.2. Minerals in the Partings

In comparison with the mineral matter in the coal benches, the four partings (YLT6U-2p, YLT6U-9p, YLT6L-3p and YLT6L-4p) have lower calcite and higher kaolinite and mixed-layer illite/smectite contents. In addition, the partings within the YLT6U coal have higher anatase and lower quartz contents. The partings within the YLT6L coal have higher chlorite and lower pyrite contents relative to those in the respective coal benches (Table 2, Figure 4). XRD analysis of the fractions of the partings shows relatively more abundant kaolinite and I/S, with small proportion of quartz, chamosite and berthierine in the clay mineral assemblage (Figure 9A–D). The chamosite is represented by a peak at 14.4 Å under air-dried conditions in sample YLT6L-4p, and its peak of 7.1 Å appears on heating (Figure 9D). Authigenic kaolinite and mixed-layer illite/smectite in the partings occur as fusinite- and semifusinite-cell fillings (Figure 10A), as vermicular form (Figure 10B,C) and as a matrix (Figure 10D). Kaolinite and mixed-layer illite/smectite (I/S) also occur as discrete particles (Figure 10E,F) and, in some cases, are distributed along bedding planes (Figure 10G).

Chlorite in the partings occurs generally as a cryptocrystalline matrix coexisting with anatase and pyrite (Figure 11A,C). Anatase provides Ti peaks in some of the chlorite EDS spectrum (Figure 10K). A small proportion of epigenetic chlorite occurs as fracture-filling in sample YLT6L-4p (Figure 11B). Chlorite with sub-angular forms (Figure 10F,J) formed because earlier formed apatite was chloritized by Fe-Mg fluids.

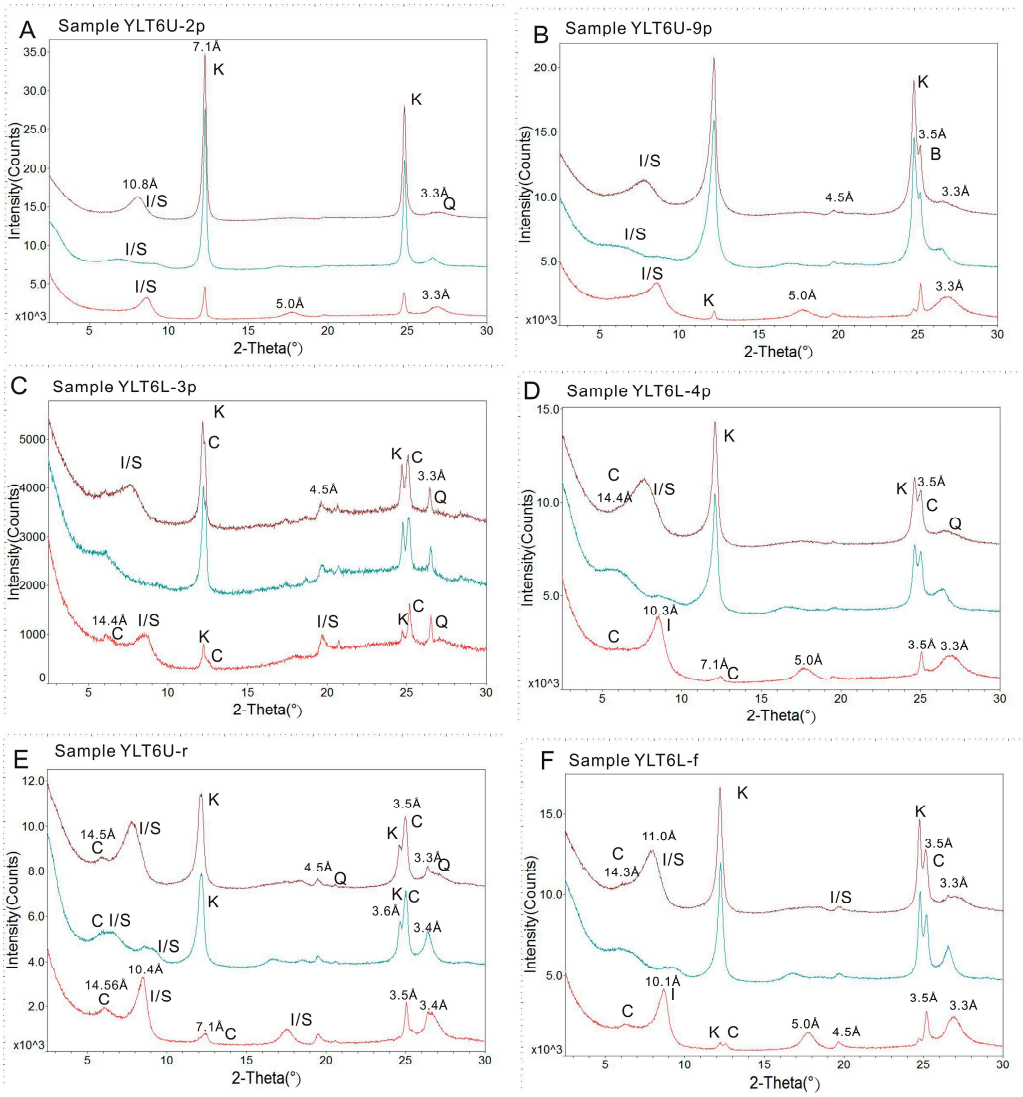

Figure 9. X-ray diffractogram (XRD) patterns of clay-fractions. (**A**) Sample YLT6U-2p; (**B**) sample YLT6U-9p; (**C**) sample YLT6L-3p; (**D**) sample YLT6L-4p; (**E**) sample YLT6U-r; (**F**) sample YLT6L-f. K, kaolinite; I/S, mixed-layer illite/smectite; C, chamosite; B, berthierine; Q, quartz. Natural-oriented (top trace), glycol-saturated (middle trace) and heated (bottom trace). Numbers represent d-spacings in Ångstrom units.

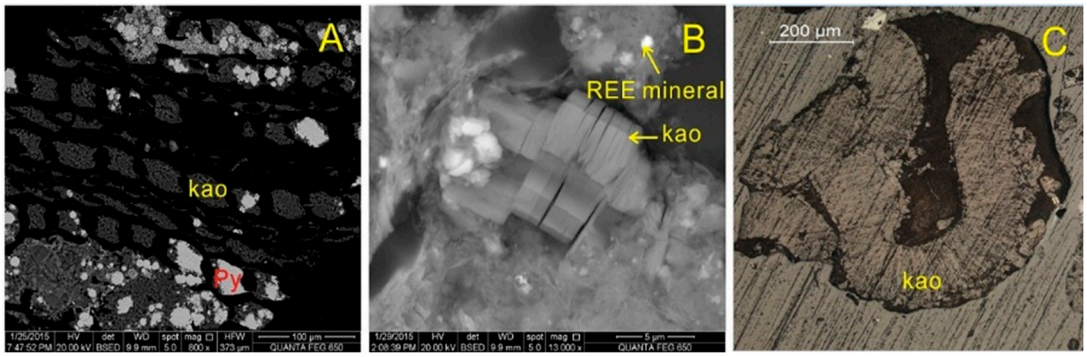

Figure 10. *Cont*.

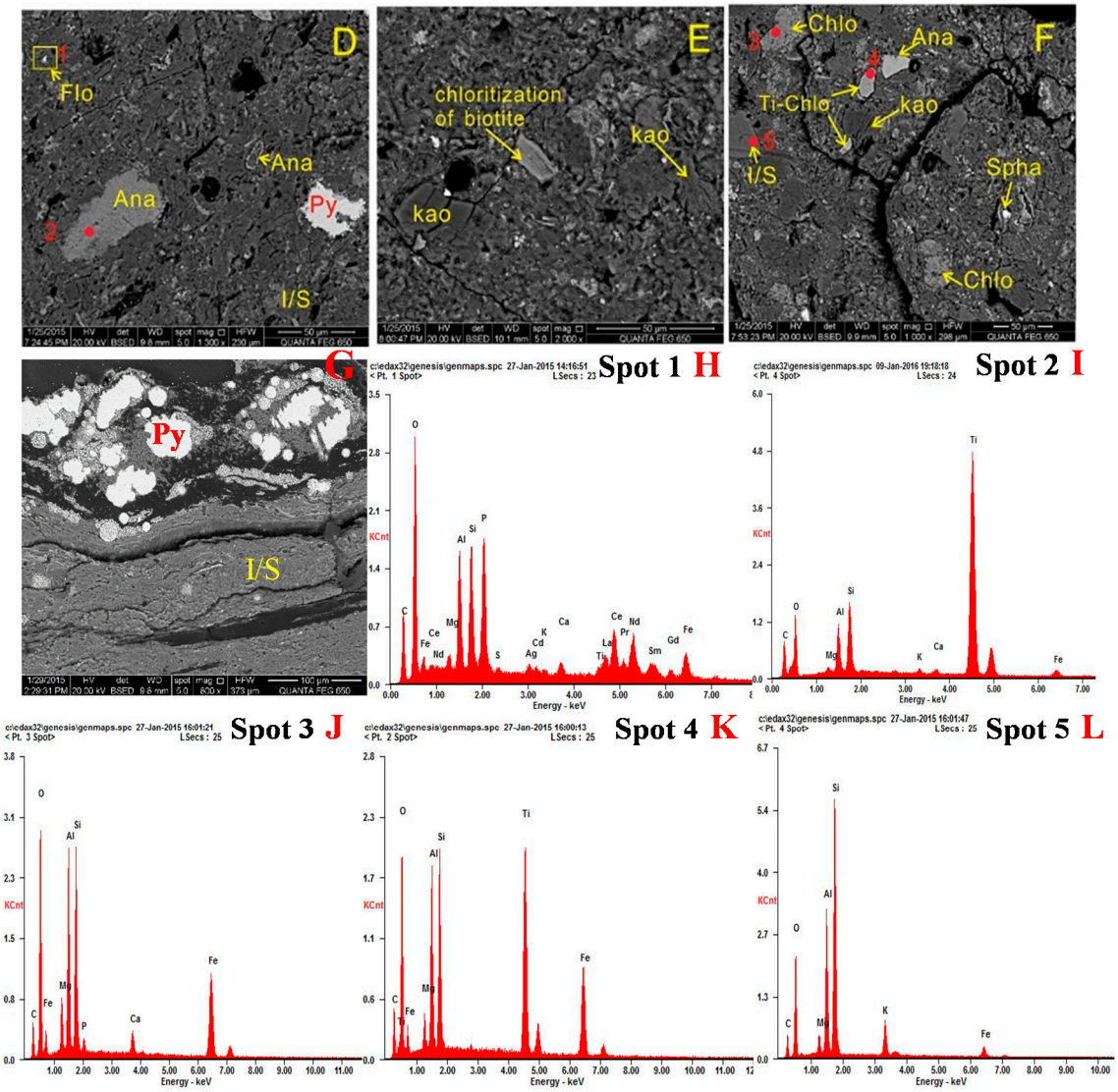

Figure 10. Reflected white light optical microscope, SEM back-scattered electron images and selected EDS data in YLT6U and YLT6L partings. (**A**) Fusinite- and semifusinite-cell filling kaolinite and pyrite in sample YLT6L-4p; (**B**) Vermicular kaolinite in sample YLT6U-9p; (**C**) Vermicular kaolinite in sample YLT6U-2p (optical microscope); (**D**) Anatase, I/S, pyrite and monazite in sample YLT6L-4p; (**E**) Kaolinite and chloritized biotite in sample YLT6L-4p; (**F**) I/S, Kaolinite, anatase, sphalerite and chlorite in sample YLT6L-4p; (**G**) Mixed-layer I/S distributed along the bedding planes in sample YLT6U-9p. Sample YLT6L-4p is carbon coated, and sample YLT6U-9p is detected under low vacuum without coating. (**H**–**L**) EDS spectra of Spots 1–5. Kao, kaolinite; Py, pyrite; Ana, anatase; Chlo, chlorite; Flo, florencite; Spha, sphalerite.

Anatase in the partings occurs as coarse-crystalline (Figure 11A,B) and beaded form (Figures 10D and 11D). They were closely associated with clay minerals and were probably precipitated from Ti-rich fluids with Ti leaching from volcanic ash as described below. The blocky and framboidal pyrite, associated with some fragments of organic matter in sample YLT6U-9p (Figure 10G), suggests that the pyrite is a syngenetic sedimentary material rather than a derivation of volcanic ash. Euhedral pyrite of syngenetic origin also occurs as cubes and octahedrons (Figure 11E). Cell- and cavity-filling pyrite (Figures 10A and 11F) in the YLT6L coal is of authigenic origin.

A number of accessory minerals have also been found in the partings. Epigenetic barite occurs as fracture fillings (Figure 11G), and in some cases, it also coexists with mixed-layer I/S (Figure 11H).

Lathlike sphalerite is embedded in mixed-layer I/S (Figure 11I), suggestive of epigenetic origin. Monazites are present in YLT6L-4p and YLT6U-9p samples (Figure 10B,D). The Energy Dispersive X-ray Spectroscopy (EDS) spectra of minerals in Figure 11 are shown in Figure 12.

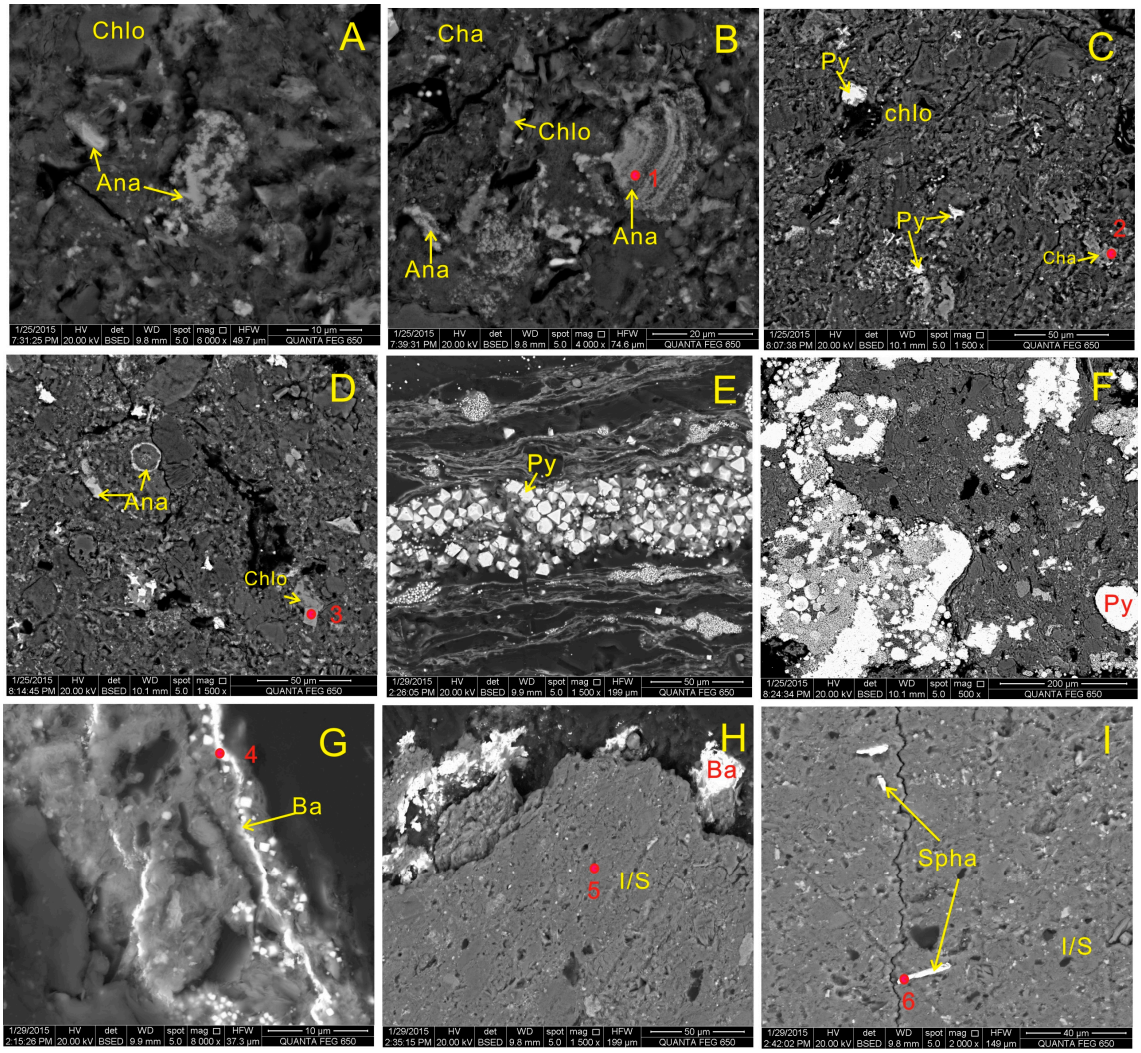

Figure 11. SEM back-scattered electron images in YLT6U and YLT6L partings. (**A**) Chlorite in sample YLT6L-4p; (**B**) fracture- and cavity-filling chlorite in sample YLT6L-4p; (**C**) chlorite in sample YLT6L-4p; (**D**) beaded anatase in sample YLT6L-4p; (**E**) euhedral pyrite in sample YLT6U-9p; (**F**) framboidal and cavity-filling pyrite in sample YLT6L-4p; (**G**) fracture-filling barite in sample YLT6U-9p; (**H**) barite coexisting with I/S in sample YLT6U-9p; (**I**) sphalerite in sample YLT6U-9p. Py, pyrite; Ana, anatase; Chlo, chlorite; Cha, chamosite; Ba, barite; Spha, sphalerite.

The roof of the YLT6U coal (YLT6U-r) and the floor of the YLT6L coal (YLT6L-f) are macroscopically and microscopically different. Macroscopically, sample YLT6L-f shows a well-developed bedding plane compared to sample YLT6U-r. Microscopically, samples YLT6U-r and YLT6L-f are mainly composed of mixed-layer illite/smectite and quartz, with a lesser proportion of chlorite, anatase and calcite (Table 2, Figure 4). Siderite and muscovite are also present in sample YLT6U-r, and kaolinite, pyrite and apatite are present in the floor of the YLT6L coal. The clay minerals identified in the host rocks by the clay-fraction studies are kaolinite, chamosite and mixed-layer I/S (Figure 9E,F). The mixed-layer I/S in sample YLT6L-f has a peak of 11.0 Å on the natural-oriented aggregate. The sharp peak of 10.1 Å in sample YLT6L-f indicates the presence of illite on heated aggregate (Figure 9F).

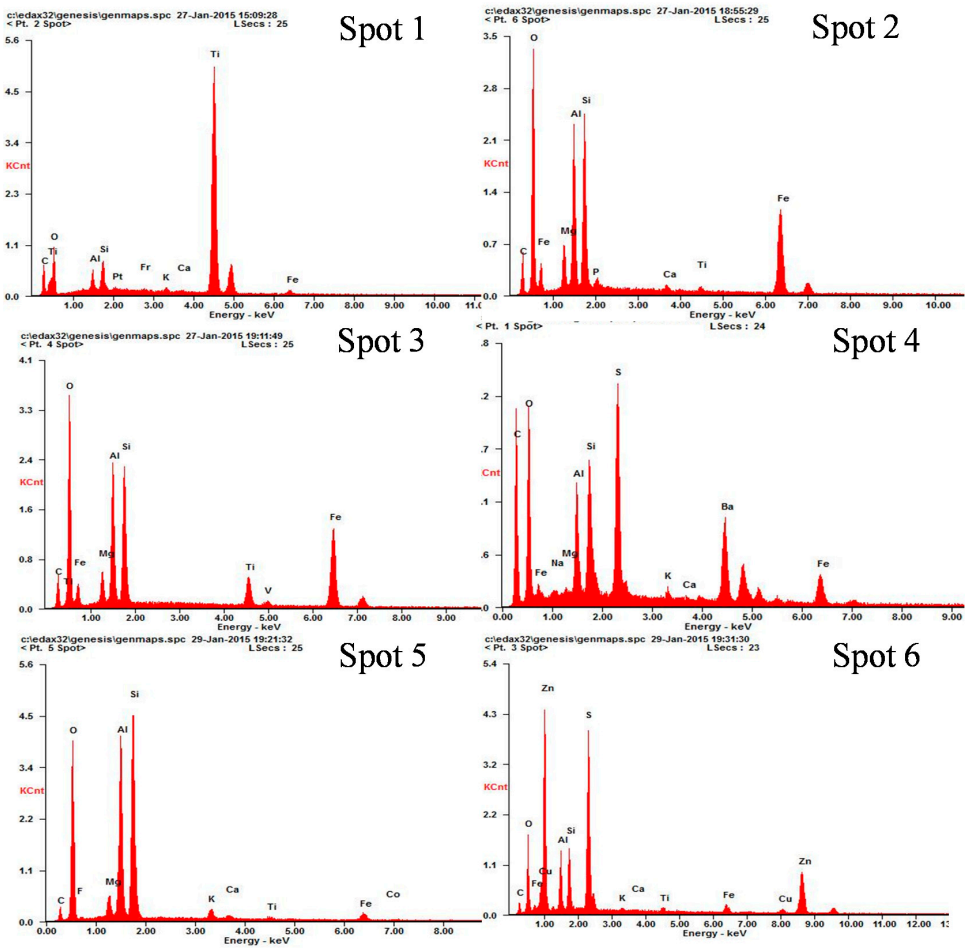

Figure 12. EDS spectra of Spots 1–6 in Figure 11.

Quartz in the host rocks occurs mainly as discrete particles with irregular forms (Figure 13A,B). Kaolinite in sample YLT6L-f occurs as discrete particles (Figure 13B,C), and some kaolinite has flocculent shapes (Figure 13D,E). Authigenic anatase in the host rocks is ring shaped (Figure 13A) or occurs as discrete particles (Figure 13B), coarse-crystalline (Figure 13D), platy (Figure 13E), linear (Figure 13F) and fracture-infilling (Figure 13G,H) forms. In addition, some anatases coexist with stripped apatite (Figure 13H). Chamosite coexisting with kaolinite in flocculent forms (Figure 13D,E,H) occurs in the roof strata. Euhedral pyrite is present in the floor (Figure 13I), suggestive of syngenetic origin.

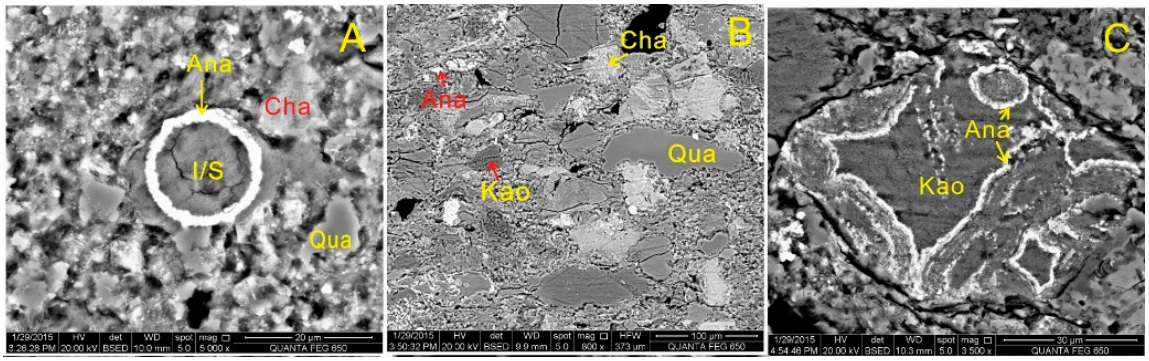

Figure 13. *Cont.*

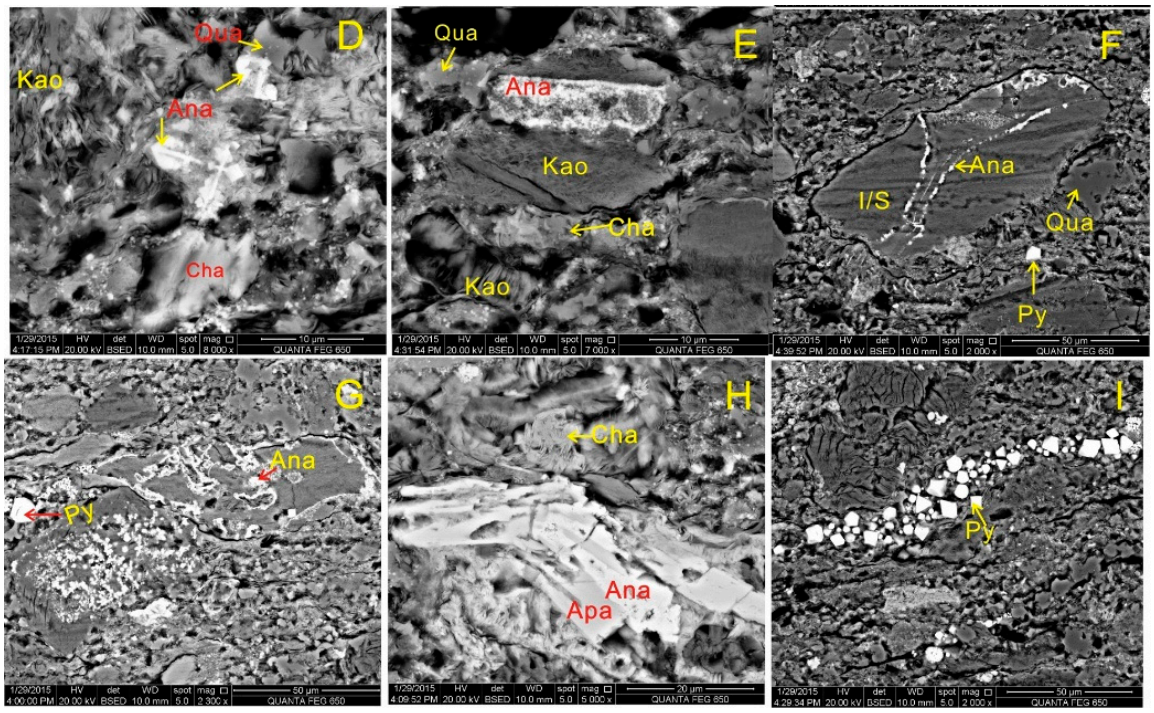

Figure 13. SEM back-scattered electron images in the host rocks (under low vacuum). (**A**) Quartz, I/S, chamosite and ring-shaped anatase in sample YLT6U-r; (**B**) Quartz, kaolinite, anatase and chamosite in sample YLT6L-f; (**C**) Kaolinite and anatase in sample YLT6L-f; (**D**) Flocculent kaolinite, anatase and chamosite in sample YLT6L-f; (**E**) Kaolinite and chamosite in sample YLT6L-f; (**F**) Anatase and pyrite in sample YLT6L-f; (**G**) Fracture-filling anatase and pyrite in sample YLT6L-f; (**H**) Anatase, chamosite and apatite in sample YLT6L-f; (**I**) Euhedral pyrite in sample YLT6L-f. Kao, kaolinite; Py, pyrite; Ana, anatase; Cha, chamosite; Qua, quartz; Apa, apatite.

5. Discussion

The assemblage of minerals in the No. 6 coal seam of the Yueliangtian coals and associated non-coal samples is attributed to four factors, including sediment-source region, multi-stage injections of hydrothermal fluids, seawater influence and volcanic ash input.

5.1. Sediment-Source Region Influence

Similar to other Late Permian coals from southwestern China [36,43–45], the Kangdian Upland (Figure 1) is the sediment-source region for the YLT6 coal [11]. Not only the Emeishan mafic basalts, but also the overlying felsic-intermediate rocks could have been the terrigenous source materials for the Late Permian coals present in this study [46]. Quartz in the YLT6 coal is slightly higher than that in coals from the Dafang (0.8%–11.4% on average) [14] and Zhijin (0.5%–9.4% on average) mines [35] (Figure 1), consistent with Dai *et al.* [15] and indicating that the closer the coals are located to the sediment-source Kangdian Upland region, the higher the quartz in the coal. The abundant authigenic quartz (Figure 5A) is precipitated from the silica-bearing solutions from the weathering of basalt in the Kangdian Upland [15,47,48].

Although the thick lava sequence from the Emeishan large igneous province in southwestern China is basalt, silicic rocks also occur in the uppermost part of the Kangdian upland [47]. There is no quartz and apatite in Emeishan basalt of the Kangdian Upland [49]; the abundant detrital quartz (Figure 5B–D) and authigenic apatite (Figure 13H) probably indicate that the parent rock is also granite or other silicic rocks [47].

5.2. Multi-Stage Injections of Hydrothermal Fluids

Hydrothermal fluids play an important role in the enrichment of minerals and trace elements in the coals of Guizhou province [5,12,14,41]. Multi-stage hydrothermal fluids also influenced the mineralogical characteristics of the Yueliangtian coals, partings, roof and floor.

The cell-filling kaolinite (Figure 7A,B) suggests an authigenic origin in coal. Al- and Si-bearing solutions from the sediment-source Kangdian Upland region precipitated in the cells of coal-forming plants during coal formation. Although chlorite (e.g., chamosite) is rare in coals, if present, it is usually observed in high-rank coals or in coals influenced by epigenetic hydrothermal solutions [44,50,51]. Chamosite is present in the YLT6 coal and coexists with kaolinite and quartz (Figure 13D,E) in the roof strata. As suggested by Equation (1), the earlier-precipitated kaolinite was invaded by Fe-Mg-rich hydrothermal fluids and generated kaolinite and chamosite during early diagenesis at temperatures around 165–200 °C [52]. Then, kaolinite and chamosite desilicated and generated quartz, as suggested by Equation (2). Dispersed chamosite (Figure 13B) independent of kaolinite and quartz may have precipitated from Fe-rich hydrothermal solutions, with Fe probably coming from siderite layers in the sedimentary sequence (Figure 2) [53].

$$\text{Kaolinite} + \text{Fe} + \text{Mg} \rightarrow \text{Kaolinite} + \text{Chamosite}\,(165 - 200\,^{\circ}\text{C}) \quad (1)$$

$$\text{Kaolinite} + \text{Chamosite} \rightarrow \text{Chamosite} + \text{Quartz}\,(\text{Desilication}) \quad (2)$$

The abundant authigenic quartz (Figure 5A) is probably precipitated from the silicious solution of the weathering product of Emeishan basalt from the Kangdian Upland [47,54]. Epigenetic vein-like calcite (Figure 6D) is probably precipitated by the circulation of Ca-bearing meteoric fluids or by Ca-rich solutions during the coal-formation process [55]. The average formation temperature of vein calcite is about 190 °C [14].

The crystal-shaped cavities commonly occurred in the samples YLT6L-4p (Figures 10D,E and 11C,D) and YLT6L-f (Figure 13E), suggesting that the earlier formed mineral crystals were corroded by hydrothermal solutions [15].

The modes of occurrence of coarse-crystalized anatase (YLT6L-4p; Figure 11A,B), cell-filling calcite (YLT6U-6; Figure 6A), fracture-filling barite (YLT6U-9p; Figure 11G) and cell- or fracture-filling pyrite (YLT6L-4p; Figures 10A and 11F) also suggest solution deposition during different stages of the coal formation [15,41].

5.3. Seawater Influence

Although the vertical distance between the floor of the YLT6U and the roof of the YLT6L coals is only 2.94 m, the deposit environments of the two coals are strikingly different.

The total sulfur contents (ranging from 3.61%–13.34%) in the YLT6L coal are higher than those in the YLT6U coal (0.27%–0.75%). Except for the YLT6U-8 and YLT6U-9p samples, no pyrite was present in the YLT6U coal. However, pyrite of syngenetic origin is common in the YLT6L coal, non-coal partings and floor strata (Figure 8B,D,E, Figures 10G, 11E and 13I). It can be inferred that seawater provided a sulfur source both during peat forming and in the diagenetic process of the YLT6L coal. The abundant calcite and mixed-layer I/S in the YLT6L coal also signifies the alkaline, medium environment of seawater (Table 2), which are also beneficial for calcite formation and the transformation from kaolinite to mixed-layer I/S [4]. The paleoenvironment of the Longtan Formation varies from lagoons and tidal flats [11–14]. Thus, seawater had a tremendous influence on YLT6L coal and terminated at the YLT6U-9p sampling interval.

5.4. Volcanic Ash Input

As described by Spears [56,57], Dai *et al.* [58,59], Zhou *et al.* [60] and Zhao *et al.* [43], "tonsteins" are partings derived from air-borne material of pyroclastic origin in the peat-forming environment. They have been found in some coal seams of SW China [15,43,58–60].

The three partings (samples YLT6U-2p, YLT6U-9p and YLT6L-4p) have a lateral continuity within the Yueliangtian coal mine. As shown in Table 2, the mineralogy of the three non-coal partings is dominated by kaolinite and mixed-layer I/S, accounting for 80%–89.1% of the mineral compositions of the respective parting. The mixed-layer I/S in the partings mostly occurs as cryptocrystalline matrix (Figures 10D and 11H,I). Kaolinite in samples YLT6U-2p and YLT6U-9p occurs as large crystals with a well-developed vermicular texture (Figure 10B,C). Vermicular kaolinite is thought to indicate air-fall volcanic ash layers altered and deposited in a non-marine, coal-forming environment [61]. Biotite pseudomorphs with chlorite laminae occur in the sample YLT6L-4p (Figure 10E). Such an occurrence of chloritized biotite suggests an *in situ* crystallized origin [15].

High-temperature quartz has been identified in the sample YLT6L-f. The β-quartz (Figure 13B) present in this study shows triangle and irregular forms and is considered to have originated from autochthonous syngenetic felsic to intermediate volcanic ashes. Dai *et al.* [59] and Zhou *et al.* [60] suggested that tonsteins in the lower and upper portions of the Late Permian were mainly of alkali and felsic composition, respectively. The No. 6 coal seam in the present study is located in the upper portion of the Late Permian strata (Figure 2).

The modes of anatase occurrence in the partings (Figure 11D) and floor strata (Figure 13A,F) suggest that it probably either was altered by pyroxene crystals in the original volcanic ash or reprecipitated after labile components was chemically leached in the original volcanic ash [15].

Zircon was not observed by optical microscope or SEM in the tonsteins of the present study, probably either because the relevant volcanic ashes did not contain this mineral phases or because multi-stage hydrothermal fluids as mentioned above altered it.

The mineral assemblages and occurrences of mineral of partings and roof strata in the No. 6 coal seam of the Yueliangtian coal mine suggest that the three partings (samples YLT6U-2p, YLT6U-9p and YLT6L-4p) and roof strata appear to have been derived from felsic volcanic ash.

6. Conclusions

(1) The major mineral phases in the YLT6U and YLT6L coals are calcite, quartz, kaolinite and pyrite and, to a lesser extent, chlorite, anatase, illite, mixed-layer illite/smectite, rutile, bassanite and ankerite. The Emeishan basalt and silicic rocks in the Kangdian Upland are the parent rocks of the Yueliangtian coals.

(2) Different modes of occurrence of chamosite are present in the YLT6 coal. This, accompanied with cell-filling quartz, pyrite, and calcite veins, suggests that multi-stage hydrothermal fluids influenced the Yueliangtian coals.

(3) The sedimentary environment is different between the YLT6U and YLT6L coals. Seawater had a tremendous influence on the YLT6L coal and terminated at the YLT6U-9p sampling interval.

(4) Three tonstein (samples YLT6U-2p, YLT6U-9p and YLT6L-4p) layers identified in the coal are probably derived from felsic volcanic ash. These tonsteins are characterized by the occurrence of vermicular kaolinite and chloritized biotite. The roof strata of the YLT6L coal also appear to have been derived from felsic volcanic ash.

Acknowledgments: This research was supported by the National Key Basic Research Program of China (No. 2014CB238902), the National Natural Science Foundation of China (Nos. 41420104001 and 41272182), and the Program for Changjiang Scholars and Innovative Research Team in University (IRT13099). The authors are grateful to three anonymous reviewers and editor for their careful comments, which greatly improved the paper quality. We would like to thank Shifeng Dai and Lei Zhao for their constructive suggestions on the earlier version of this paper.

Author Contributions: Panpan Xie designed the overall experimental strategy and participated in all of the experiments. Hongjian Song has performed the XRD experiments. Jianpeng Wei and Qingqian Li analyzed the minerals in the samples using SEM-EDX. All authors participated in writing the manuscript.

Conflicts of Interest: The authors declare no conflict of interest.

References

1. Dai, S.F.; Ren, D.Y.; Chou, C.-L.; Finkelman, R.B.; Seredin, V.V.; Zhou, Y.P. Geochemistry of trace elements in Chinese coals: A review of abundances, genetic types, impacts on human health, and industrial utilization. *Int. J. Coal Geol.* **2012**, *94*, 3–21. [CrossRef]
2. Liu, J.J.; Yang, Z.; Yan, X.Y.; Ji, D.P.; Yang, Y.C.; Hu, L.C. Modes of occurrence of highly-elevated trace elements in superhigh-organic-sulfur coals. *Fuel* **2015**, *156*, 190–197. [CrossRef]
3. Dai, S.F.; Ren, D.Y.; Zhou, Y.P.; Chou, C.-L.; Wang, X.B.; Zhao, L.; Zhu, X.W. Mineralogy and geochemistry of a superhigh-organic-sulfur coal, Yanshan Coalfield, Yunnan, China: Evidence for a volcanic ash component and influence by submarine exhalation. *Chem. Geol.* **2008**, *255*, 182–194. [CrossRef]
4. Shao, Y.B.; Guo, Y.H.; Qin, Y.; Shen, Y.L.; Tian, L. Distribution characteristic and geological significance of rare earth elements in Lopingian mudstone of Permian, Panxian county, Guizhou province. *Min. Sci. Technol.* **2011**, *21*, 469–476. [CrossRef]
5. Zhang, J.Y.; Ren, D.Y.; Zheng, C.G.; Zeng, R.S.; Chou, C.-L.; Liu, J. Trace element abundances in major minerals of Late Permian coals from southwestern Guizhou province, China. *Int. J. Coal Geol.* **2002**, *53*, 55–64. [CrossRef]
6. Xiao, K. Analysia of principles for geological structures of Yueliangtian Coal Mine. *Min. Saf. Environ. Prot.* **2003**, *30*, 25–26.
7. Dai, S.F.; Chekryzhov, I.Y.; Seredin, V.V.; Nechaev, V.P.; Graham, I.T.; Hower, J.C.; Ward, C.R.; Ren, D.Y.; Wang, X.B. Metalliferous coal deposits in East Asia (Primorye of Russia and South China): A review of geodynamic controls and styles of mineralization. *Gondwana Res.* **2016**, *29*, 60–82. [CrossRef]
8. Dai, S.F.; Seredin, V.V.; Ward, C.R.; Hower, J.C.; Xing, Y.W.; Zhang, W.G.; Song, W.J.; Wang, P.P. Enrichment of U-Se-Mo-Re-V in coals preserved within marine carbonate successions: Geochemical and mineralogical data from the Late Permian Guiding Coalfield, Guizhou, China. *Miner. Deposita* **2015**, *50*, 159–186. [CrossRef]
9. Ward, C.R. Analysis and significance of mineral matter in coal seams. *Int. J. Coal Geol.* **2002**, *50*, 135–168. [CrossRef]
10. Yuan, M.; Zhang, F. Structure formation and its application to coal exploration in south No. 4 Mining Field, Yueliangtian Coal Mine. *Coal Geol. Explor.* **2004**, *4*, 16–18.
11. Coal Geology Bureau of China. *Sedimentary Environments and Coal Accumulation of Late Permian Coal Formation in Western Guizhou, Southern Sichuan and Eastern Yunnan, China*; Chongqing University Press: Chongqing, China, 1996. (In Chinese)
12. Dai, S.F.; Ren, D.Y.; Tang, Y.G.; Shao, L.Y.; Hao, L.M. Influences of low-temperature hydrothermal fluid on the re-distributions and occurrences of associated elements in coal—A case study from the Late Permian coals in the Zhijin Coalfield, Guizhou Province, southern China. *Acta Geol. Sin.* **2002**, *76*, 437–445.
13. Dai, S.F.; Ren, D.Y.; Tang, Y.G.; Yue, M.; Hao, L.M. Concentration and distribution of elements in Late Permian coals from western Guizhou Province, China. *Int. J. Coal Geol.* **2005**, *61*, 119–137. [CrossRef]
14. Dai, S.F.; Chou, C.-L.; Yue, M.; Luo, K.L.; Ren, D.Y. Mineralogy and geochemistry of a Late Permian coal in the Dafang Coalfield, Guizhou, China: Influence from siliceous and iron-rich calcic hydrothermal fluids. *Int. J. Coal Geol.* **2005**, *61*, 241–258. [CrossRef]
15. Dai, S.F.; Li, T.; Seredin, V.V.; Ward, R.C.; Hower, J.C.; Zhou, Y.P.; Zhang, M.Q.; Song, X.L.; Song, W.J.; Zhao, C.L. Origin of minerals and elements in the Late Permian coals, tonsteins, and host rocks of the Xinde Mine, Xuanwei, eastern Yunnan, China. *Int. J. Coal Geol.* **2014**, *121*, 53–78. [CrossRef]
16. Coal Analysis Laboratory of China Coal Research Institute. *Chinese Standard Method GB/T 482-2008, Sampling of Coal Seams*; National Coal Standardization Technical Committee: Beijing, China, 2008.
17. ASTM International. *Test Method for Moisture in the Analysis Sample of Coal and Coke*; ASTM D3173-11; ASTM International: West Conshohocken, PA, USA, 2011.
18. ASTM International. *Test Method for Volatile Matter in the Analysis Sample of Coal and Coke*; ASTM D3175-11; ASTM International: West Conshohocken, PA, USA, 2011.

19. ASTM International. *Test Method for Ash in the Analysis Sample of Coal and Coke from Coal*; ASTM D3174-11; ASTM International: West Conshohocken, PA, USA, 2011.
20. ASTM International. *Test Methods for Total Sulfur in the Analysis Sample of Coal and Coke*; ASTM D3177-02; ASTM International: West Conshohocken, PA, USA, 2011.
21. ASTM International. *Standard Practice for Preparing Coal Samples for Microscopical Analysis by Reflected Light*; ASTM Standard D2797/D2797M-11a; ASTM International: West Conshohocken, PA, USA, 2011.
22. ASTM International. *Standard Test Method for Microscopical Determination of the Vitrinite Reflectance of Coal*; ASTM Standard D2798-11a; ASTM International: West Conshohocken, PA, USA, 2011.
23. Rietveld, H.M. A profile refinement method for nuclear and magnetic structures. *J. Appl. Crystal.* **1969**, *2*, 65–71. [CrossRef]
24. Taylor, J.C. Computer programs for standardless quantitative analysis of minerals using the full powder diffraction profile. *Powder Diffr.* **1991**, *6*, 2–9. [CrossRef]
25. Ward, C.R.; Spears, D.A.; Booth, C.A.; Staton, I.; Gurba, L.W. Mineral matter and trace elements in coals of the Gunnedah Basin, New South Wales, Australia. *Int. J. Coal Geol.* **1999**, *40*, 281–308. [CrossRef]
26. Ward, C.R.; Matulis, C.E.; Taylor, J.C.; Dale, L.S. Quantification of mineral matter in the Argonne Premium coals using interactive Rietveld-based X-ray diffraction. *Int. J. Coal Geol.* **2001**, *46*, 67–82. [CrossRef]
27. Ruan, C.D.; Ward, C.R. Quantitative X-ray powder diffraction analysis of clay minerals in Australian coals using Rietveld methods. *Appl. Clay Sci.* **2002**, *21*, 227–240. [CrossRef]
28. Dai, S.F.; Yang, J.Y.; Ward, C.R.; Hower, J.C.; Liu, H.D.; Garrison, T.M.; French, D.; O'Keefe, J.M.K. Geochemical and mineralogical evidence for a coal-hosted uranium deposit in the Yili Basin, Xinjiang, northwestern China. *Ore Geol Rev.* **2015**, *70*, 1–30. [CrossRef]
29. Dai, S.F.; Wang, P.P.; Ward, C.R.; Tang, Y.G.; Song, X.L.; Jiang, J.H.; Hower, J.C.; Li, T.; Seredin, V.V.; Wagner, N.J.; *et al*. Elemental and mineralogical anomalies in the coal-hosted Ge ore deposit of Lincang, Yunnan, southwestern China: Key role of N_2-CO_2-mixed hydrothermal solutions. *Int. J. Coal Geol.* **2014**, *152*, 19–46. [CrossRef]
30. Dai, S.F.; Zhang, W.G.; Ward, C.R.; Seredin, V.V.; Hower, J.C.; Li, X.; Song, W.J.; Wang, X.B.; Kang, H.; Zheng, L.C.; *et al*. Mineralogical and geochemical anomalies of late Permian coals from the Fusui Coalfield, Guangxi province, southern China: Influences of terrigenous materials and hydrothermal fluids. *Int. J. Coal Geol.* **2013**, *105*, 60–84. [CrossRef]
31. China Southwest Oil and Gas Field Company Exploration and Development Institute. *Chinese Petrol and Naturl Gas Industry Standard SY/T 5163-2010, Analysis Method for Clay Minerals and Ordinary Non-Clay Minerals in Sedimentary Rocks by the X-ray Diffraction*; Petroleum Exploration Standardization Technical Committee: Beijing, China, 2010. (In Chinese)
32. ASTM International. *Standard Classification of Coals by Rank*; ASTM D388-12; ASTM International: West Conshohocken, PA, USA, 2012.
33. Coal Analysis Laboratory of China Coal Research Institute. *Chinese Standard Method GB/T 15224.1-2010, Classification for Quality of Coal. Part 1: Ash*; Standardization Administration of China: Beijing, China, 2010. (In Chinese)
34. Dai, S.F.; Ren, D.Y.; Hou, X.Q.; Shao, L.Y. Geochemical and mineralogical anomalies of the late Permian coal in the Zhijin coalfield of southwest China and their volcanic origin. *Int. J. Coal Geol.* **2003**, *55*, 117–138. [CrossRef]
35. Dai, S.F.; Li, D.H.; Ren, D.Y.; Tang, Y.G.; Shao, L.Y.; Song, H.B. Geochemistry of the late Permian No. 30 coal seam, Zhijin Coalfield of Southwest China: Influence of a siliceous low-temperature hydrothermal fluid. *Appl. Geochem.* **2004**, *19*, 1315–1330. [CrossRef]
36. Zhuang, X.G.; Querol, X.; Zeng, R.S.; Xu, W.D.; Alastuy, A.; Lopez-Soler, A.; Plana, F. Mineralogy and geochemistry of coal from the Liupanshui mining district, Guizhou, south China. *Int. J. Coal Geol.* **2000**, *45*, 21–37. [CrossRef]
37. Dai, S.F.; Wang, X.B.; Chen, W.M.; Li, D.H.; Chou, C.-L.; Zhou, Y.P.; Zhu, C.S.; Li, H.; Zhu, X.Y.; Xing, Y.W.; *et al*. A high-pyrite semianthracite of late Permian age in the Songzao Coalfield, southwestern China: Mineralogical and geochemical relations with underlying mafic tuffs. *Int. J. Coal Geol.* **2010**, *83*, 430–445. [CrossRef]

38. Widodo, S.; Oschmann, W.; Bechtel, A.; Sachsenhofer, R.F.; Anggayana, K.; Puettmann, W. Distribution of sulfur and pyrite in coal seams from Kutai Basin (east Kalimantan, Indonesia): Implications for paleoenvironmental conditions. *Int. J. Coal Geol.* **2010**, *81*, 151–162. [CrossRef]
39. Dai, S.F.; Hou, X.Q.; Ren, D.Y.; Tang, Y.G. Surface analysis of pyrite in the No. 9 coal seam, Wuda coalfield, Inner Mongolia, China, using high-resolution time-of-flight secondary ion mass-spectrometry. *Int. J. Coal Geol.* **2003**, *55*, 139–150. [CrossRef]
40. Dai, S.F.; Ren, D.Y.; Tang, Y.G.; Shao, L.Y.; Li, S.S. Distribution, isotopic variation and origin of sulfur in coals in the Wuda coalfield, Inner Mongolia, China. *Int. J. Coal Geol.* **2002**, *52*, 237–250. [CrossRef]
41. Yang, J.Y. Modes of occurrence and origins of noble metals in the Late Permian coals from the Puan Coalfield, Guizhou, southwest China. *Fuel* **2006**, *85*, 1679–1684. [CrossRef]
42. Chou, C.-L. Sulfur in coals: A review of geochemistry and origins. *Int. J. Coal Geol.* **2012**, *100*, 1–13. [CrossRef]
43. Zhao, L.; Ward, C.R.; French, D.; Graham, I.T. Mineralogical composition of Late Permian coal seams in the Songzao Coalfield, southwestern China. *Int. J. Coal Geol.* **2013**, *116–117*, 208–226. [CrossRef]
44. Dai, S.F.; Tian, L.W.; Chou, C.-L.; Zhou, Y.; Zhang, M.Q.; Zhao, L.; Wang, J.M.; Yang, Z.; Cao, H.Z.; Ren, D.Y. Mineralogical and compositional characteristics of Late Permian coals from an area of high lung cancer rate in Xuan Wei, Yunnan, China: Occurrence and origin of quartz and chamosite. *Int. J. Coal Geol.* **2008**, *76*, 318–327. [CrossRef]
45. Dai, S.F.; Zhou, Y.P.; Ren, D.Y.; Wang, X.B.; Li, D.; Zhao, L. Geochemistry and mineralogy of the Late Permian coals from the Songzo Coalfield, Chongqing, southwestern China. *Sci China Ser. D Earth Sci.* **2007**, *50*, 678–688. [CrossRef]
46. Dai, S.F.; Liu, J.J.; Ward, C.R.; Hower, J.C.; French, D.; Jia, S.H.; Hood, M.M.; Garrison, T.M. Mineralogical and geochemical compositions of Late Permian coals and host rocks from the Guxu coalfield, Sichuan Province, China, with emphasis on enrichment of rare metals. *Int. J. Coal Geol.* **2015**. [CrossRef]
47. Wang, X.B.; Wang, R.X.; Wei, Q.; Wang, P.P.; Wei, J.P. Mineralogical and geochemical characteristics of Late Permian coals from the Mahe Mine, Zhaotong Coalfield, Northeastern Yunnan, China. *Mineral* **2015**, *5*, 380–396. [CrossRef]
48. Ren, D.Y. Mineral matter in coal. In *Coal Petrology of China*; Han, D.X., Ed.; Publishing House of China University of Mining and Technology: Xuzhou, China, 1996; pp. 67–78. (In Chinese)
49. Xu, Y.G.; Chung, S.L.; Jahn, B.M.; Wu, G.Y. Petrologic and geochemical constraints on the petrogenesis of Permian-Triassic Emeishan flood basalts in southwestern China. *Lithos* **2001**, *58*, 145–168. [CrossRef]
50. Permana, A.K.; Ward, C.R.; Li, Z.; Gurba, L.W. Distribution and origin of minerals in high-rank coals of the South Walker Creek area, Bowen Basin, Australia. *Int. J. Coal Geol.* **2013**, *116–117*, 185–207. [CrossRef]
51. Dai, S.F.; Chou, C.-L. Occurrence and origin of minerals in a chamosite-bearing coal of Late Permian age, Zhaotong, Yunnan, China. *Am. Mineral.* **2007**, *92*, 1253–1261. [CrossRef]
52. Boles, J.R.; Franks, S.G. Clay diagenesis in Wilcox sandstones of southwest Texas: Implications of smectite diagenesis on sandstone cementation. *J. Sediment. Res.* **1979**, *49*, 55–70.
53. Iijima, A.; Matsumoto, R. Berthierine and chamosite in coal measures of Japan. *Clay Clay Miner.* **1982**, *30*, 264–274. [CrossRef]
54. Wang, X.B.; Dai, S.F.; Chou, C.-L.; Zhang, M.Q.; Wang, J.M.; Song, X.L.; Wang, W.; Jiang, Y.F.; Zhou, Y.P.; Ren, D.Y. Mineralogy and geochemistry of Late Permian coals from the Taoshuping Mine, Yunnan Province, China: Evidences for the sources of minerals. *Int. J. Coal Geol.* **2012**, *96–97*, 49–59. [CrossRef]
55. Kolker, A.; Chou, C.-L. Cleat-filling calcite in Illinois Basin coals: Trace element evidence for meteoric fluid migration in a coal basin. *J. Geol.* **1994**, *102*, 111–116. [CrossRef]
56. Spears, D.A.; Kanaris-Sotiriou, R. A geochemical and mineralogical investigation of some British and other European tonsteins. *Sedimentology* **1979**, *26*, 407–425. [CrossRef]
57. Spears, D.A. The origin of tonsteins, an overview, and links with seatearths, fireclays and fragmental clay rocks. *Int. J. Coal Geol.* **2012**, *94*, 22–31. [CrossRef]
58. Dai, S.F.; Luo, Y.B.; Seredin, V.V.; Ward, C.R.; Hower, J.C.; Zhao, L.; Liu, S.D.; Zhao, C.L.; Tian, H.M.; Zou, J.H. Revisiting the Late Permian coal from the Huayingshan, Sichuan, southwestern China: Enrichment and occurrence modes of minerals and trace elements. *Int. J. Coal Geol.* **2014**, *122*, 110–128. [CrossRef]
59. Dai, S.F.; Wang, X.B.; Zhou, Y.P.; Hower, J.C.; Li, D.H.; Chen, W.M.; Zhu, X.W.; Zou, J.H. Chemical and mineralogical compositions of silicic, mafic, and alkali tonsteins in the Late Permian coals from the Songzao Coalfield, Chongqing, Southwest China. *Chem. Geol.* **2011**, *282*, 29–44. [CrossRef]

60. Zhou, Y.P.; Bohor, B.F.; Ren, Y. Trace element geochemistry of altered volcanic ash layers (tonsteins) in Late Permian coal-bearing formations of eastern Yunnan and western Guizhou Provinces, China. *Int. J. Coal Geol.* **2000**, *44*, 305–324. [CrossRef]
61. Bohor, B.F.; Triplehorn, D.M. Tonsteins: Altered volcanic-ash layers in coal-bearing sequences. *Geol. Soc. Am. Spec. Pap.* **1993**, *285*, 1–44.

© 2016 by the authors; licensee MDPI, Basel, Switzerland. This article is an open access article distributed under the terms and conditions of the Creative Commons by Attribution (CC-BY) license (http://creativecommons.org/licenses/by/4.0/).